Synchrotron x-ray diffraction and DFT study of non-centrosymmetric EuRhGe$_3$ under high pressure

N. S. Dhami, V. Balédent, I. Batistić, O. Bednarchuk, D. Kaczorowski, J. P. Itié, S. R. Shieh, C. M. N. Kumar & Y. Utsumi

➕ View supplementary material ↗

📅 Published online: 04 Sep 2024.

✎ Submit your article to this journal ↗

🔍 View related articles ↗

View Crossmark data ↗

Check for updates

Synchrotron x-ray diffraction and DFT study of non-centrosymmetric EuRhGe₃ under high pressure

N. S. Dhami[a], V. Balédent[b], I. Batistić[c], O. Bednarchuk[d], D. Kaczorowski[d], J. P. Itié[e], S. R. Shieh[f], C. M. N. Kumar[g] and Y. Utsumi[a]

[a]Department for Research of Materials Under Extreme Conditions, Institute of Physics, Zagreb, Croatia; [b]Université Paris-Saclay, CNRS, Laboratoire de Physique des Solides, Orsay, France; [c]Department of Physics, Faculty of Science, University of Zagreb, Zagreb, Croatia; [d]Institute of Low Temperature and Structure Research, Polish Academy of Sciences, Wrocław, Poland; [e]PSICHÉ beamline, Synchrotron SOLEIL, Saint-Aubin, France; [f]Department of Earth Sciences, Department of Physics and Astronomy, University of Western Ontario, London, Ontario, Canada; [g]Department of Molecular Magnetism, The Henryk Niewodniczański, Institute of Nuclear Physics, Polish Academy of Sciences, Kraków, Poland

ABSTRACT

Antiferromagnetic intermetallic compound EuRhGe₃ crystalizes in a non-centrosymmetric BaNiSn₃-type ($I4\,mm$) structure. We studied its pressure-dependent crystal structure by using synchrotron powder x-ray diffraction at room temperature. Our results show a smooth contraction of the unit cell volume by applying pressure while preserving $I4\,mm$ symmetry. No structural transition was observed up to 35 GPa. By the equation of state fitting analysis, the bulk modulus and its pressure derivative were determined to be 73 (1) GPa and 5.5 (2), respectively. Furthermore, similar to the isostructural EuCoGe₃, an anisotropic compression of a and c lattice parameters was observed. Our experimental results show a good agreement with the pressure-dependent structural evolution expected from theoretical calculations below 13 GPa. Reflecting a strong deviation from integer Eu valence, the experimental volume data appear to be smaller than those of DFT calculated values at higher pressures.

1. Introduction

Rare-earth compounds in non-centrosymmetric BaNiSn₃-type structures have attracted considerable attention for their rich magnetic properties and pressure-induced superconductivity [1]. A series of Eu-based silicides/germanides EuTX_3 (T = transition metal, X = Si or Ge) have been discovered with the BaNiSn₃-type structure. In the crystallographic unit cell of EuTX_3 systems, Eu atoms occupy the 2a Wyckoff site, silicon/germanium atoms are located at two different Wyckoff positions 2a and 4b, while transition metal atoms occupy the 2a site [2,3]. Due to the lack of inversion symmetry in the crystal structure, the Dzyaloshinskii-Moriya antisymmetric spin interaction plays an active role and results in complex magnetic structures among the EuTX_3 series [3–8].

EuRhGe$_3$ possesses magnetic Eu^{2+} (4f^7, $J = 7/2$) ions and exhibits antiferromagnetic ordering in the tetragonal *ab*-plane below $T_N = 11.3$ K [3,4]. Temperature-dependent electrical resistivity of EuRhGe$_3$ shows a linear increase of T_N by applying pressure up to 8 GPa [9]. Since the energy difference between Eu^{2+} and nonmagnetic Eu^{3+} (4f^6, $J = 0$) is not very large [10], and the ionic radius of Eu^{3+} is ~10% smaller than Eu^{2+} ion, a pressure-induced Eu valence transition accompanied by a collapse of antiferromagnetic ordering and a volume change was expected. This phenomenon has been observed in ternary Eu-compounds with the ThCr$_2$Si$_2$-type (*I4/mmm*) structure [11,12]. However, the antiferromagnetic ordering and divalent Eu were revealed to be stable against pressure in EuRhGe$_3$. Recently, we performed high energy resolution fluorescence detected (HERFD) near-edge x-ray absorption spectroscopy (XAS) on EuRhGe$_3$ as a function of pressure. In the Eu L_3-edge XAS spectra, a prominent Eu^{2+} peak was observed at ambient pressure. By increasing pressure, the spectral intensity shifted from Eu^{2+} to Eu^{3+} peaks. The obtained mean Eu valence from the Eu L_3 XAS spectrum exhibited a continuous increase from ~2.1 at ambient pressure to ~2.4 at 40 GPa without a first-order valence transition [13].

Pressure-dependent Eu valence and crystal structure were also studied in isostructural antiferromagnets EuCoGe$_3$ and EuNiGe$_3$. Their antiferromagnetic phases are stable against pressure [9,14,15]. Both exhibited a continuous contraction of their unit cell volume by applying pressure without any symmetry changes [16,17]. The mean Eu valence in EuCoGe$_3$ only changes from 2.2 at 2 GPa to ~2.3 even around 50 GPa [16]. In EuNiGe$_3$, the mean Eu valence changes from 2.13 at 1 GPa to 2.43 at 48 GPa at 8 K [17]. As well as EuRhGe$_3$, the Eu valence does not reach Eu^{3+} in both EuNiGe$_3$ and EuCoGe$_3$, even under such high pressure. These pressure-dependent changes of Eu valence in the Eu*T*Ge$_3$ series are rather small compared to ternary Eu-compounds with the ThCr$_2$Si$_2$-type structure (Eu122-systems), which often show a drastic pressure-induced Eu valence transition below 10 GPa [11,12]. For example, antiferromagnet EuRh$_2$Si$_2$ exhibits a pressure-induced valence transition at room temperature. By applying pressure, the mean Eu valence changes from Eu$^{2.2+}$ at ambient pressure to almost Eu^{3+} at ~8 GPa [18]. Such pressure-induced valence transition is also reported in antiferromagnet EuNi$_2$Ge$_2$, where the Eu valence changes from 2.2 at ambient pressure to almost Eu^{3+} above 5 GPa at room temperature [19]. In the Eu122-systems, a correlation between the Eu valence and its unit cell volume tends to appear as a lattice volume collapse simultaneously happening with the Eu valence transition since the size of the Eu^{3+} ion is about 10% smaller than the Eu^{2+} ion [20].

The different pressure behavior in the Eu*T*Ge$_3$ series from the Eu122-systems raises questions about whether the variation of the Eu valence in the Eu*T*Ge$_3$ series correlates with the pressure evolution as well as their crystal structural changes. Unlike the intensively investigated Eu122-systems, pressure-dependent crystal structural studies of the Eu*T*Ge$_3$ series remain scarce. To elucidate a trend of pressure-dependent structural changes in the Eu*T*Ge$_3$ series and its relation to the Eu valence evolutions, a systematic study is needed. Here we performed synchrotron powder x-ray diffraction (XRD) as a function of pressure to study the pressure-dependent crystal structural change in EuRhGe$_3$, together with the theoretical predictions by density functional theory (DFT) method. The results are discussed in relation to the pressure evolution of the mean Eu valence obtained by HERFD near-edge XAS [13].

2. Experiment

Single crystals of $EuRhGe_3$ were synthesized by the metal-flux method using liquid indium as solvent. The crystals were taken from the same batch reported in Ref. [3]. The grown crystals were characterized by XRD, electrical resistivity, and magnetic susceptibility measurement [3–5].

The high-resolution XRD was performed at the PSICHE beamline of SOLEIL synchrotron with a photon energy of 33 keV ($\lambda = 0.3738$ Å). The single crystal of $EuRhGe_3$ was ground into a powder using mortar and pestle with ethanol. Fine grains of $EuRhGe_3$ afloat on the ethanol were collected by using a syringe and transferred onto a clean glass slide. After drying the powdered sample was loaded in a membrane diamond anvil cell (DAC). Diamonds of 300 μm diameter culet size were used. A rhenium gasket was pre-indented to about 28 μm thickness, and then a hole of 150 μm was drilled through it to serve as a sample chamber. Gold powder was also loaded in the DAC as a pressure reference material. Helium was used as a pressure-transmitting medium. Pressure was controlled by a membrane on the DAC and was determined by the Au equation of state [21].

The pressure evolution of the crystal structure of $EuRhGe_3$ was also studied theoretically by using the Quantum ESPRESSO DFT package [22,23]. In DFT calculations, we have used pseudopotentials from pslibrary 1.0.0 [24], with the Perdew–Burke–Ernzerhof exchange-correlation functional appropriate for solids [25,26]. The kinetic energy cutoff for wavefunctions was 150 Ry, while for the charge density and potential, it was 700 Ry. The Brillouin sampling was $16 \times 16 \times 8$ (no offset), with the Marzari–Vanderbilt Fermi surface smearing [27]. To take into account the antiferromagnetic ordering on Eu, we have used the simplified formulation of DFT+U proposed by Dudarev [28]. The Hubbard interaction U for Eu was assumed to be 3.8 eV to match the Eu 4f peak in the valence band spectrum by photoelectron spectroscopy measurement [29]. This U value was kept constant for all pressure calculations.

3. Results and discussion

We performed powder XRD on $EuRhGe_3$ as a function of pressure at room temperature up to 35 GPa. The contour map of diffraction intensities in the pressure range from 1 to 35 GPa is presented in Figure 1. In order to highlight the pressure evolution of the peak positions, the contour map is plotted in the 2θ range from 5 to 19 deg. The pressure evolution of Bragg peak positions contains the main phase $EuRhGe_3$ and gold as pressure reference. When pressure exceeds 25 GPa, new peaks that belong to neither $EuRhGe_3$ nor gold emerge in the diffraction pattern. These new peaks were identified as rhenium from the gasket.

We integrated the diffraction images using Dioptas software [30] and performed Rietveld refinement for three phases using the Profex program [31]. The Rietveld refinement fits at selected pressures are presented in Figure 2. Although the DAC was prepared not to have an excessive amount of the sample in the gasket hole, a possible occurrence of bridging between the diamond anvils cannot be eliminated, which could explain the broadening of the diffraction peaks above 10 GPa. Note that, helium pressure medium has the highest hydrostatic limit among other rare gases [32], a development of uniaxial stress is reported above 30 GPa that largely depends on experiments [33,34]. The obtained lattice
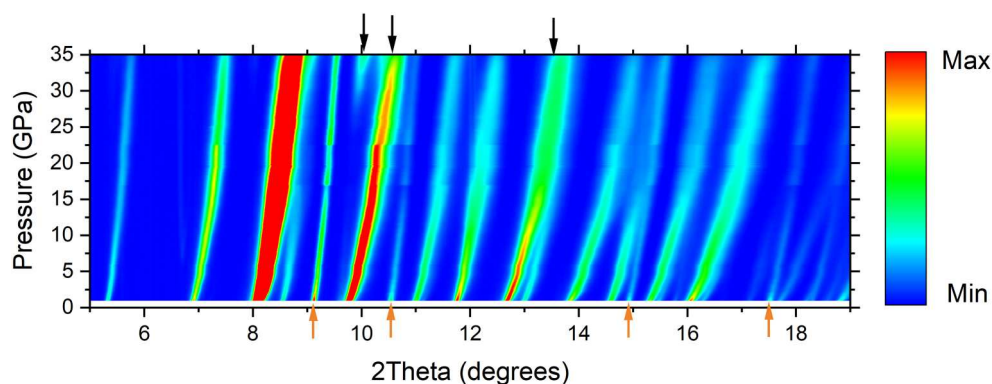
Figure 1. Contour map of synchrotron x-ray diffraction intensities in the pressure range 1–35 GPa. The pressure evolution of Bragg peak positions contains EuRhGe$_3$ (main phase), gold (standard material), and rhenium (gasket) which appears above 25 GPa. The black arrows (top) and yellow arrows (bottom) indicate the main peak positions of rhenium and gold respectively.

parameters and refinement parameters at selected pressures are shown in Table 1. The detailed atomic coordinates as a function of pressure are presented in Appendix 2. Our analysis confirms that EuRhGe$_3$ maintains the same crystal symmetry ($I4\,mm$) up to 35 GPa. Note that the unit cell parameters $a = 4.4129$ Å, $c = 10.0906$ Å, and unit cell volume $V_0 = 196.50$ Å^3 at ambient pressure are taken from Ref. [3].

Figure 3(a) shows the evolution of lattice parameters a and c as a function of pressure. The lattice parameter a shows greater pressure change compared to c. Similar high-pressure behavior is also observed in EuCoGe$_3$ [16] and EuNiGe$_3$ [17]. We also performed high-pressure powder XRD of EuRhGe$_3$ by using a neon pressure transmitting medium. The pressure-dependent changes of a and c lattice parameters showed the same tendency (see supporting material), which suggests an intrinsic pressure behavior to the EuTGe$_3$ series and is independent from the pressure medium. Figure 3(b) shows the
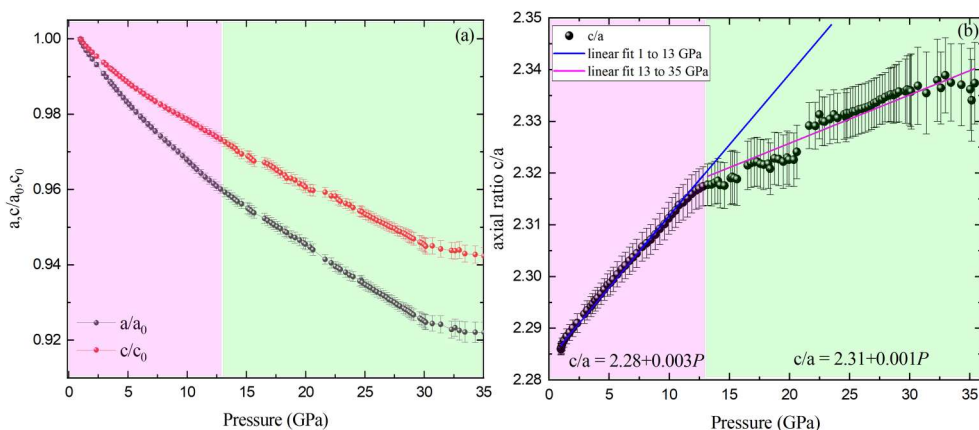
Table 1. Experimental lattice parameters, unit cell volume, and refinement parameters of EuRhGe$_3$ at selected pressures.

Pressure	1 GPa	10 GPa	25 GPa	35 GPa
(Experimental) Lattice parameters and volume				
a (Å)	4.3899 (1)	4.249 (4)	4.103 (2)	4.04 (1)
c (Å)	10.035 (3)	9.821 (9)	9.567 (6)	9.45 (2)
V (Å^3)	193.38 (9)	177.3 (3)	161.1 (1)	154.2 (8)
Refinement parameters				
R_{WP}	9.47	10.39	9.8	9.21
R_{exp}	10.11	9.55	9.98	10.52
χ^2	0.88	1.17	0.96	0.77
GOF	0.94	1.06	0.98	0.91
Pressure	0 GPa	10 GPa	20 GPa	30 GPa
(DFT) Lattice parameters and volume				
a (Å)	4.3889	4.2547	4.1564	4.0774
c (Å)	10.0478	9.8246	9.6787	9.5731
V (Å^3)	193.5452	177.8495	167.2059	159.1546

Note: Where R_{WP} is the weighted profile R factor, R_{exp} is the expected R factor and GOF is the goodness of fitting. Lattice parameters and unit cell volume obtained by DFT calculation at various pressures.
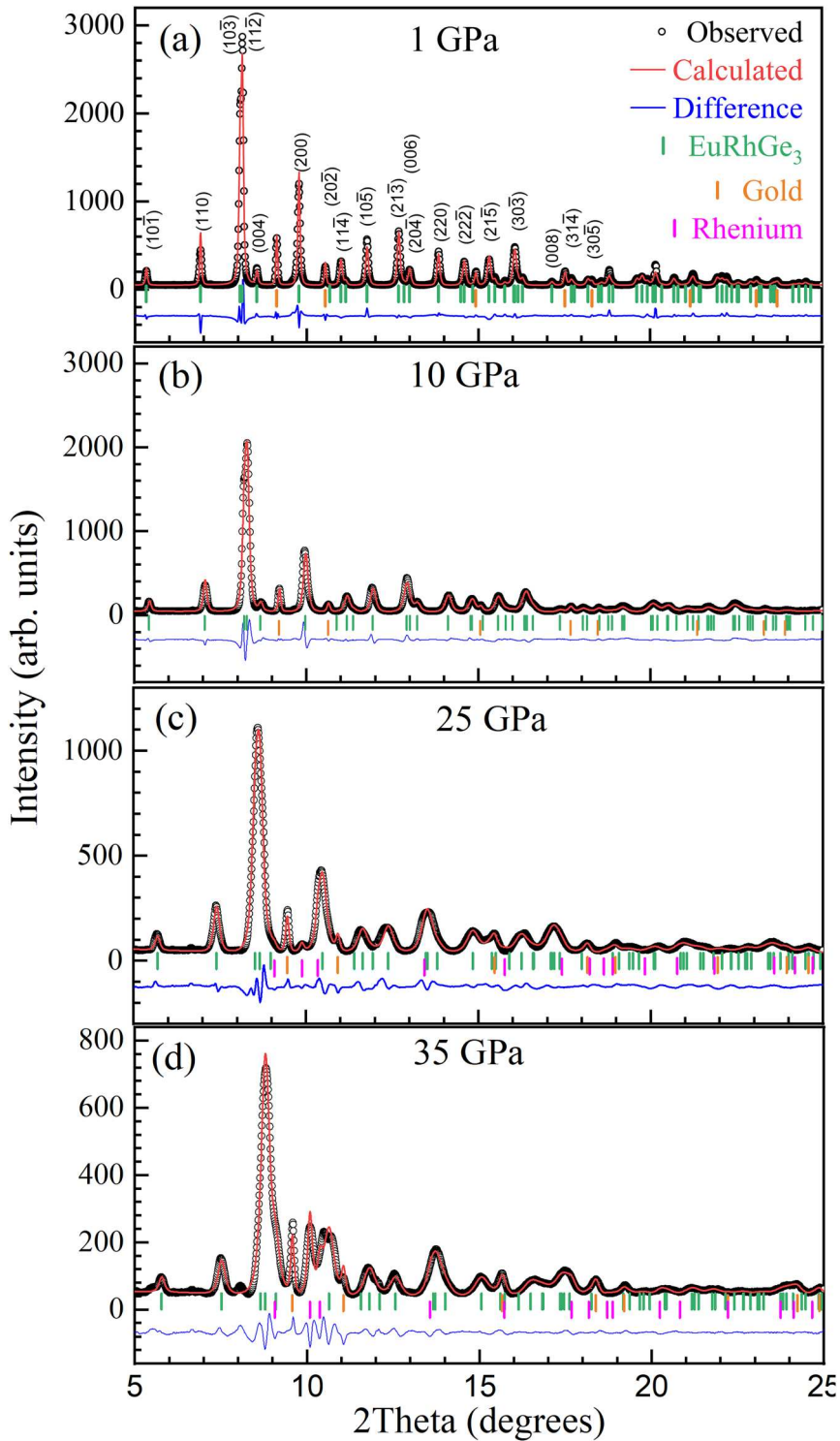
Figure 2. Synchrotron powder XRD patterns of EuRhGe$_3$ along with the results of Rietveld refinement at (a) 1 GPa, (b) 10 GPa, (c) 25 GPa, and (d) 35 GPa. The vertical bars indicate Bragg peak positions of EuRhGe$_3$ (green), gold (orange), and rhenium (magenta).

Figure 3. (a) Relative pressure variations of the lattice parameters of EuRhGe$_3$ with respect to the values at the lowest experimental pressure. (b) Pressure dependence of the axial ratio (c/a). Straight lines emphasize linear behavior. The two different colors represent two different pressure regions. To emphasize the change of slope, the linear fit of the LP region is extended into the HP region.

change of axial ratio (c/a) as a function of pressure. Pressure evolution of the c/a can be divided into two regions: low-pressure (LP) region <13 GPa and high-pressure (HP) region above 13 GPa. The linear fitting of the LP region provides 2.28+0.003P, while it provides 2.31+0.001P in the HP region. In the LP region, the value of the c/a linearly increases with pressure with a rate of 0.003 GPa^{-1}, then the rate decreases to 0.001 GPa^{-1} in the HP region. This change in the c/a increase rate is ascribed to a change in compressibility along the a- and c-axis. The linear modulus of the c-axis increases considerably in the HP region, which makes the c-axis less compressible and changes the slope of c/a (see Appendix 1). Among Eu122-systems, the change of c/a slope as a function of pressure was reported as a consequence of pressure-induced isostructural transition. Across such isostructural transition from tetragonal to so-called collapsed tetragonal phase, a-, c-lattice parameters and the unit cell volume greatly change along with the c/a slope [19,35–38]. Compared to the large structural changes in Eu122-systems, no discontinuous changes are observed in lattice parameters at the pressure range of the c/a slope change in EuRhGe$_3$. Moreover, the c/a slope change does not coincide with the pressure change of Eu valence in EuRhGe$_3$. The isostructural phase transitions in the Eu122-systems are accompanied by pressure-induced Eu valence transition from almost Eu^{2+} to Eu^{3+}. However, in EuRhGe$_3$, the mean Eu valence linearly increases from ~2.1 at ambient pressure to ~2.4 around 25 GPa, then the increase rate becomes smaller and deviates from the linear behavior above 25 GPa [13]. Hence, we eliminate the possibility of pressure-induced isostructural transition in EuRhGe$_3$. It is worth mentioning that the change of the c/a slope as a function of pressure was also observed in EuCoGe$_3$ [16] and EuNiGe$_3$ [17] without any isostructural transitions.

Figure 4 shows the pressure evolution of the unit cell volume of EuRhGe$_3$. It exhibits a smooth contraction with increasing pressure. A slight change in the slope can be seen around 30 GPa (also in the lattice parameters of Figure 3(a)). This slope change of the unit cell volume coincides with the slope change of the mean Eu valence as a function
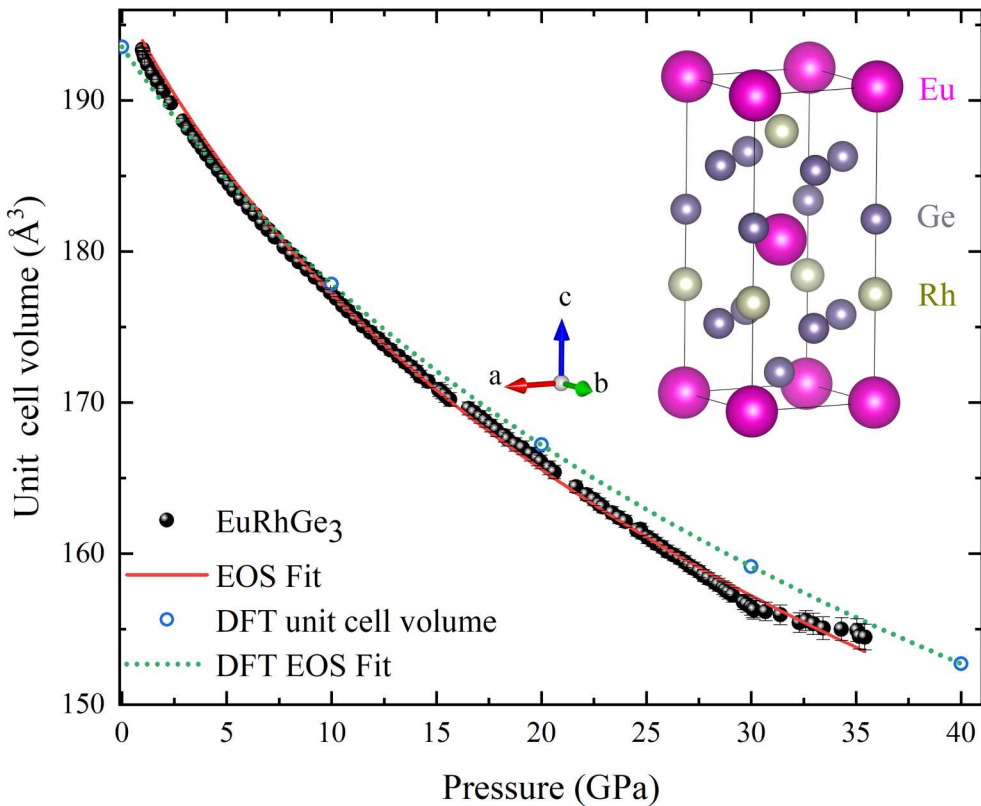
Figure 4. Pressure evolution of the unit cell volume of $EuRhGe_3$ (solid circles) with the result of EOS fitting (solid line). The unit cell volume obtained by DFT calculation for the selected pressures (open circles) and its EOS fitting (dashed line). The error bar is the range of symbol size. The inset shows the crystal structure of $EuRhGe_3$ drawn by VESTA [41].

of pressure. The mean Eu valence of $EuRhGe_3$ obtained by HERFD XAS exhibited a linear increase by applying pressure up to 25 GPa and exhibited a smaller change at higher pressure [13]. Pressure-dependent unit cell volumes obtained by the DFT calculation are also plotted in Figure 4. The theoretically calculated unit cell volumes exhibit a good agreement with experimental results in the LP region. However, the deviation from the experimental results increases in the HP region. The DFT-calculated unit cell volumes in the HP region tend to be larger than the experimental values. This is due to the change of the *c*-axis compressibility in the HP region, which is not captured by the DFT calculation. Since the DFT calculations cannot take into account the valence fluctuation, the Eu valence was considered to be Eu^{2+} in the whole pressure range. In the LP range, the average Eu valence in $EuRhGe_3$ stayed close to Eu^{2+} (2.1–2.2) [13] resulting in a reasonable agreement between the experiment and the DFT calculation. However, the mean Eu valence increases toward 2.4 by further increasing pressure. Considering the different ionic radius between Eu^{2+} and Eu^{3+} (10% smaller), it is somewhat understandable that the experimental unit cell volume appears to be smaller than the DFT-calculated values. In order to study the elastic properties of $EuRhGe_3$, we performed

Table 2. The unit cell volumes, bulk modulus, and first pressure derivative of bulk modulus of EuTGe$_3$ series and those obtained by the DFT calculation in EuRhGe$_3$.

Compound	Unit cell volume (V_0)	Bulk modulus (B_0)	B'_0
EuCoGe$_3$	184.39 (Å^3)	75.6	5.58 [16]
EuNiGe$_3$	185.7 (Å^3)	79	8.8 [17]
EuRhGe$_3$ (XRD)	196.50 (Å^3)	73 (1)	5.5(2)
EuRhGe$_3$ (DFT)	193.545 (Å^3)	97.4(1)	4.61(1)

Note: The values of EuCoGe$_3$ and EuNiGe$_3$ are taken from Ref. [16,17], respectively.

equation of state (EOS) fitting by using EOSFit7c software [39]. We used the 3rd order Birch Murnaghan equation below for EOS fitting [40] :

$$P(V) = \frac{3B_0}{2} \left[\left(\frac{V_0}{V}\right)^{7/3} - \left(\frac{V_0}{V}\right)^{5/3} \right] \left\{ 1 + \frac{3}{4}(B'_0 - 4) \left[\left(\frac{V_0}{V}\right)^{2/3} - 1 \right] \right\}$$

Here, B_0 and B'_0 denote the bulk modulus at 0 GPa and its first pressure derivative, respectively. We also performed EOS fitting on the lattice volume of EuRhGe$_3$ obtained by the DFT calculation. The obtained values from the EOS fitting are listed in the Table 2 and compared with the reported values of EuCoGe$_3$ and EuNiGe$_3$, as well as those obtained in the theoretical unit cell volume of EuRhGe$_3$.

4. Conclusion

We performed pressure-dependent synchrotron x-ray diffraction measurements on polycrystalline non-centrosymmetric EuRhGe$_3$ at room temperature. It revealed a smooth contraction of the lattice constants without any structural transition within the investigated pressure range. An anisotropic compressibility between the a- and c-axis was observed. The lattice parameter along the a-axis exhibits more sensitivity to pressure and greater contraction in comparison to that of the c-axis. The change of slope in the pressure-dependent c/a ratio was observed around 13 GPa, which does not seem to have a direct correspondence to the pressure evolution of the mean Eu valence in EuRhGe$_3$. By performing the EOS fitting on the obtained unit cell volume, we determined the bulk modulus and its pressure derivative of EuRhGe$_3$. Our experimental results show a good agreement with the pressure-dependent structural changes expected from the DFT calculations at P<13 GPa, and slightly deviates in the HP region. The experimental unit cell volume tends to be smaller than the theoretical values in the HP region as a consequence of the increased mean Eu valence in the HP region.

Disclosure statement

No potential conflict of interest was reported by the author(s).

Funding

References

[1] Smidman M, Salamon MB, Yuan HQ, et al. Superconductivity and spin–orbit coupling in non-centrosymmetric materials: a review. Rep Prog Phys. 2017 Jan;80(3):036501. doi: 10.1088/1361-6633/80/3/036501

[2] Kaczorowski D, Belan B, Gladyshevskii R. Magnetic and electrical properties of eupdge3. Solid State Commun. 2012;152(10):839–841. doi: 10.1016/j.ssc.2012.02.022

[3] Bednarchuk O, Gągor A, Kaczorowski D. Synthesis, crystal structure and physical properties of eutge3 (t =co, ni, rh, pd, ir, pt) single crystals. J Alloys Compd. 2015;622:432–439. doi: 10.1016/j.jallcom.2014.10.087

[4] Bednarchuk O, Kaczorowski D. Strongly anisotropic and complex magnetic behavior in eurhge3. J Alloys Compd. 2015;646:291–297. doi: 10.1016/j.jallcom.2015.06.125

[5] Bednarchuk O, Kaczorowski D. Low-temperature physical properties of single-crystalline eucoge3 and eurhge3. Acta Phys Pol A. 2015;127(2):418–420. doi: 10.12693/APhysPolA.127.418

[6] Maurya A, Bonville P, Thamizhavel A, et al. EuNiGe$_3$, an anisotropic antiferromagnet. J Phys: Condens Matter. 2014 May;26(21):216001. doi: 10.1088/0953-8984/26/21/216001

[7] Maurya A, Bonville P, Kulkarni R, et al. Magnetic properties and complex magnetic phase diagram in non-centrosymmetric eurhge3 and euirge3 single crystals. J Magn Magn Mater. 2016;401:823–831. doi: 10.1016/j.jmmm.2015.10.134

[8] Matsumura T, Tsukagoshi M, Ueda Y, et al. Cycloidal magnetic ordering in noncentrosymmetric euirge3. J Phys Soc Japan. 2022;91(7):073703. doi: 10.7566/JPSJ.91.073703

[9] Kakihana M, Akamine H, Tomori K, et al. Superconducting, fermi surface, and magnetic properties in srtge3 and eutge3 (t: transition metal) with the rashba-type tetragonal structure. J Alloys Compd. 2017;694:439–451. doi: 10.1016/j.jallcom.2016.09.287

[10] Bauminger ER, Froindlich D, Nowik I, et al. Charge fluctuations in europium in metallic eucu$_2$si$_2$. Phys Rev Lett. 1973 May;30:1053–1056. doi: 10.1103/PhysRevLett.30.1053

[11] Ōnuki Y, Nakamura A, Honda F, et al. Divalent, trivalent, and heavy fermion states in eu compounds. Philos Magazine. 2017;97(36):3399–3414. doi: 10.1080/14786435.2016.1218081

[12] Ōnuki Y, Hedo M, Honda F. Unique electronic states of eu-based compounds. J Phys Soc Japan. 2020;89(10):102001. doi: 10.7566/JPSJ.89.102001

[13] Utsumi Y, Batistić I, Balédent V, et al. Pressure evolution of the electronic structure of non-centrosymmetric EuRhGe$_3$. Electron Struct. 2021 Jul;3(3):034002. doi: 10.1088/2516-1075/ac0c27

[14] Uchima K, Arakaki N, Hirakawa S, et al. *Pressure effect on transport properties of EuNiGe$_3$*. doi: 10.7566/JPSCP.1.012015

[15] Muthu SE, Braithwaite D, Salce B, et al. Calorimetric study on eucoge3 and eurh2in8 under pressure. J Phys Soc Japan. 2019;88(7):074702. doi: 10.7566/JPSJ.88.074702

[16] Dhami N, Balédent V, Bednarchuk O, et al. Pressure evolution of electronic and crystal structure of noncentrosymmetric eucoge 3. Phys. Rev. B. 2023;107(15):155119. doi: 10.1103/PhysRevB.107.155119

[17] Chen K, Luo C, Zhao Y, et al. Evidence of the anomalous fluctuating magnetic state by pressure-driven 4f valence change in eunige3. J Phys Chem Lett. 2023;14(4):1000–1006. doi: 10.1021/acs.jpclett.2c03569

[18] Mitsuda A, Kishaba E, Fujimoto T, et al. Pressure and magnetic field effects on the valence transition of eurh2si2. Phys B: Conden Matter. 2018;536:427–431. doi: 10.1016/j.physb.2017.10.045

[19] Hesse H-J, Lübbers R, Winzenick M, et al. Pressure and temperature dependence of the eu valence in euni2ge2 and related systems studied by mössbauer effect, x-ray absorption and x-ray diffraction. J Alloys Compd. 1997;246(1):220–231. doi: 10.1016/S0925-8388(96)02467-X

[20] Shannon RD. Revised effective ionic radii and systematic studies of interatomic distances in halides and chalcogenides. Acta Crystallogr Sect A. 1976 Sep;32(5):751–767.doi: 10.1107/S0567739476001551

[21] Heinz DL, Jeanloz R. The equation of state of the gold calibration standard. J Appl Phys. 1984;55(4):885–893. doi: 10.1063/1.333139

[22] Giannozzi P, Baroni S, Bonini N, et al. Quantum espresso: a modular and open-source software project for quantum simulations of materials. J Phys: Conden Matter. 2009 Sep;21(39):395502. doi: 10.1088/0953-8984/21/39/395502

[23] Giannozzi P, Andreussi O, Brumme T, et al. Advanced capabilities for materials modelling with quantum espresso. J Phys: Conden Matter. 2017 Oct;29(46):465901. doi: 10.1088/1361-648X/aa8f79

[24] Dal Corso A. Pseudopotentials periodic table: from h to pu. Comput Mater Sci. 2014;95:337–350. doi: 10.1016/j.commatsci.2014.07.043

[25] Perdew JP, Ruzsinszky A, Csonka GI, et al. Restoring the density-gradient expansion for exchange in solids and surfaces. Phys Rev Lett. 2008 Apr;100:136406. doi: 10.1103/PhysRevLett.100.136406

[26] Perdew JP, Ruzsinszky A, Csonka GI, et al. Erratum: restoring the density-gradient expansion for exchange in solids and surfaces [phys. rev. lett. 100, 136406 (2008)]. Phys Rev Lett. 2009 Jan;102:039902. doi: 10.1103/PhysRevLett.102.039902

[27] Marzari N, Vanderbilt D, De Vita A, et al. Thermal contraction and disordering of the al(110) surface. Phys Rev Lett. 1999 Apr;82:3296–3299. doi: 10.1103/PhysRevLett.82.3296

[28] Dudarev SL, Botton GA, Savrasov SY, et al. Electron-energy-loss spectra and the structural stability of nickel oxide: an lsda+u study. Phys Rev B. 1998 Jan;57:1505–1509. doi: 10.1103/PhysRevB.57.1505

[29] Utsumi Y, Kasinathan D, Swatek P, et al. Bulk electronic structure of non-centrosymmetric Eutge_3 (t = Co, ni, rh, ir) studied by hard x-ray photoelectron spectroscopy. Phys Rev B. 2018 Mar;97:115155. doi: 10.1103/PhysRevB.97.115155

[30] Prescher C, Prakapenka VB. Dioptas: a program for reduction of two-dimensional x-ray diffraction data and data exploration. High Press Res. 2015;35(3):223–230. doi: 10.1080/08957959.2015.1059835

[31] Doebelin N, Kleeberg R. *Profex*: a graphical user interface for the rietveld refinement program *BGMN*. J Appl Crystallogr. 2015 Oct;48(5):1573–1580. doi: 10.1107/S1600576715014685

[32] Takemura K. Evaluation of the hydrostaticity of a helium-pressure medium with powder x-ray diffraction techniques. J Appl Phys. 2001;89(1):662–668. doi: 10.1063/1.1328410

[33] Takemura K. Pressure scales and hydrostaticity. High Press Res. 2007;27(4):465–472. doi: 10.1080/08957950701659767

[34] Takemura K, Dewaele A. Isothermal equation of state for gold with a he-pressure medium. Phys Rev B. 2008 Sep;78:104119. doi: 10.1103/PhysRevB.78.104119

[35] Huhnt C, Schlabitz W, Wurth A, et al. First-order phase transitions in euco 2 p 2 and srni 2 p 2. Phys Rev B. 1997;56(21):13796. doi: 10.1103/PhysRevB.56.13796

[36] Huhnt C, Schlabitz W, Wurth A, et al. First- and second-order phase transitions in ternary europium phosphides with thcr2si2-type structure. Phys B: Conden Matter. 1998;252(1):44–54. doi: 10.1016/S0921-4526(97)00904-6

[37] Bishop M, Uhoya W, Tsoi G, et al. Formation of collapsed tetragonal phase in euco2as2 under high pressure. J Phys: Conden Matter. 2010;22(42):425701.

[38] Uhoya W, Tsoi G, Vohra YK, et al. Anomalous compressibility effects and superconductivity of eufe2as2 under high pressures. J Phys: Conden Matter. 2010;22(29):292202.

[39] Angel RJ, Gonzalez-Platas J, Alvaro M. Eosfit7c and a fortran module (library) for equation of state calculations. Zeitschrift Für Kristallographie. 2014;229:405–419. doi: 10.1515/zkri-2013-1711

[40] Birch F. Finite elastic strain of cubic crystals. Phys Rev. 1947 Jun;71:809–824. doi: 10.1103/PhysRev.71.809

[41] Momma K, Izumi F. *VESTA3* for three-dimensional visualization of crystal, volumetric and morphology data. J Appl Crystallogr. 2011 Dec;44(6):1272–1276. doi: 10.1107/S0021889811038970

Appendices

Appendix 1. Linear EOS fitting

As mentioned in the main text, the pressure evolution of the *c/a* ratio can be divided into the low-pressure (LP) region <13 GPa and the high-pressure (HP) region above 13 GPa. We also performed a linear EOS fitting by using the EOSFit7c software [39]. The linear modulus is defined as:

$$M_i = -x_i \left(\frac{\partial P}{\partial x} \right)_T$$

Thus the relation between the linear modulus and the bulk modulus can be described as follows:

$$B = \left(\frac{1}{M_1} + \frac{1}{M_2} + \frac{1}{M_3} \right)^{-1}$$

Here, M_1, M_2, and M_3 are linear moduli along the *a*-axis, *b*-axis, and *c*-axis respectively. For tetragonal symmetry M_1 and M_2 are the same. The lattice parameters along the *a*- and *c*-axis at 0 GPa ($a = 4.4129$ Å, $c = 10.0906$ Å) used for the linear EOS fitting were taken from Ref. [3]. The linear EOS fitting was performed separately in the LP and the HP regions. The obtained linear moduli along the *a*- and the *c*-axis both increase in the HP region. The linear modulus in the HP region especially increases along the *c*-axis (See Table A1). The bulk modulus calculated by using the aforementioned formula is consistent with the bulk modulus extracted from the pressure-dependent unit cell volume in the main text.

Table A1. The linear modulus at 0 GPa (M_0), and first pressure derivative of linear modulus (M_0') of EuRhGe$_3$.

axis (Pressure region)	Linear moduli (M_0)	M_0'
a (LP)	179 (1)	19.9 (5)
a (HP)	205 (4)	14.2 (6)
c (LP)	182 (4)	61 (3)
c (HP)	303 (5)	16.4 (7)

Appendix 2. DFT-calculated and experimental atomic coordinates

Table A2 presents the DFT-calculated atomic coordinates, and Table A3 shows the atomic coordinates extracted from the Rietveld refinement of the XRD data.

Table A2. Atomic coordinates of EuRhGe$_3$ obtained by DFT calculation.

Atoms	Symmetry	x	y	z
		0 GPa		
Eu	2a	0.0	0.0	0.0
Rh	2a	0.0	0.0	0.3488
Ge1	4b	0.0	0.5	0.2435
Ge2	2a	0.0	0.0	0.5864
		10 GPa		
Eu	2a	0.0	0.0	0.0
Rh	2a	0.0	0.0	0.3514
Ge1	4b	0.0	0.5	0.2423
Ge2	2a	0.0	0.0	0.5886
		20 GPa		
Eu	2a	0.0	0.0	0.0
Rh	2a	0.0	0.0	0.3532
Ge1	4b	0.0	0.5	0.2412
Ge2	2a	0.0	0.0	0.5897
		30 GPa		
Eu	2a	0.0	0.0	0.0
Rh	2a	0.0	0.0	0.3547
Ge1	4b	0.0	0.5	0.2404
Ge2	2a	0.0	0.0	0.5903
		40 GPa		
Eu	2a	0.0	0.0	0.0
Rh	2a	0.0	0.0	0.3557
Ge1	4b	0.0	0.5	0.2394
Ge2	2a	0.0	0.	0.5905

Table A3. Experimental atomic coordinates of EuRhGe$_3$ extracted from the refinement of the XRD data.

Atoms	Symmetry	x	y	z
		1 GPa		
Eu	2a	0.0	0.0	0.0
Rh	2a	0.0	0.0	0.35377± 0.00044
Ge1	4b	0.0	0.5	0.24164±0.00065
Ge2	2a	0.0	0.0	0.58194±0.00078
		10 GPa		
Eu	2a	0.0	0.0	0.0
Rh	2a	0.0	0.0	0.35424±0.00055
Ge1	4b	0.0	0.5	0.24045 ±0.00085
Ge2	2a	0.0	0.0	0.58161 ±0.00055
		25 GPa		
Eu	2a	0.0	0.0	0.0
Rh	2a	0.0	0.0	0.35556±0.00085
Ge1	4b	0.0	0.5	0.2440±0.0011
Ge2	2a	0.0	0.0	0.5916±0.0013
		35 GPa		
Eu	2a	0.0	0.0	0.0
Rh	2a	0.0	0.0	0.3568±0.0021
Ge1	4b	0.0	0.5	0.2462 ±0.0011
Ge2	2a	0.0	0.0	0.593±0.0019